Thallium-rich mineralization at Jas Roux, Hautes-Alpes, France: a complex epithermal, sediment-hosted, ore-forming system

Thaliem bohaté zrudnění v Jas Roux, Hautem-Alpes, Francie: komplexní rudotvorný systém vázaný na sedimenty

(3 text-figs, 9 tabs)

ZDENEK JOHAN[1] – JOSEPH MANTIENNE[2]

[1] *BRGM, B.P. 6009, 45060, Orléans, France*
[2] *"Les Provenchères", Route d'Olivet 6, 45160 Ardon, France*

The Jas Roux deposit, which is hosted by strongly silicified Triassic sedimentary rocks, is characterized by a complex mineralization of pyrite, sphalerite, twinnite, zinckenite, andorite, stibnite, chabourneite, parapierrotite, pierrotite, smithite, laffittite, routhierite, aktashite, wakabayashilite, realgar and barite, plus four new mineral phases: (i) a phase $Pb_9Ag(Sb,As)_{13}S_{29}$ with optical properties similar to jamesonite, VHN_{25} = 165 kg/mm², a composition close to the ideal formula, and a monoclinic unit-cell with a = 17.640, b = 18.464, c = 3.967 Å, β = 90°48', V = 1292 Å³, Z = 1, D_{calc} = 5.51; (ii) a phase $Tl(As, Sb)_{10}S_{16}$ that is X-ray amorphous; (iii) a phase $Tl(Sb,As)_7S_{11}$ that is weakly anisotropic with reflectivity close to chabourneite; and (iv) a phase Ag_2SbAsS_4, representing a reaction product between smithite and chabourneite.
Hypotheses on the genesis of the deposit, based on the determined crystallization sequence, reveal similarities between the Jas Roux ore-forming system and low-temperature active geothermal brines.

Key words: thallium minerals, Pb-, Ag-sulphisalts, mercury, epithermal mineralization, Jas Roux, France

Introduction

Low-temperature hydrothermal deposits with thallium-bearing sulphides, selenides and/or sulphosalts are still rare in nature, even though new discoveries made during the last 30 years have considerably increased their number. Historically, i. e. before the Second World War, only three localities were famous for their Tl-bearing mineral parageneses: Allchar (Macedonia), the Lengenbach quarry in Binntal (Switzerland) and Skrikerum (Sweden). Recent studies of these occurrences using the electron microprobe have led to the definition of several new Tl-bearing mineral phases. In the Allchar deposit, the known Tl-bearing association comprising lorandite and vrbaite (Caye et al. 1967; Ohmasa – Nowacki 1971) has been considerably enlarged by descriptions of raguinite (Laurent et al. 1969), picotpaulite (Johan et al. 1970), parapierrotite (Johan et al. 1975), rebulite (Balić–Žunić et al. 1982), simonite (Engel et al. 1982), bernardite (Pašava et al. 1989) and jankovicite (Cvetković et al. 1995). At Lengenbach, the known hatchite and hutchinsonite assemblage has been increased by four new thallium minerals: imhofite (Burri et al. 1965; Divjakovic – Nowacki 1976), wallisite (Takéuchi et al. 1968), stalderite and edenharterite (Graeser 1988). Finally, a new chemical formula and new crystallographic data were obtained from a re-examination of the crookesite at Skrikerum (Berger 1987; Johan 1987).

Other Tl-bearing phases have been described from:

– the Jas Roux deposit (France), subject of the present article.

– the selenium-rich parageneses from uranium deposits within the Bohemian Massif (Czech Republic), in particular those of Bukov, Petrovice and Předbořice, where two new thallium minerals were discovered: bukovite (Johan – Kvaček 1971) and sabatierite (Johan et al. 1978).

– newly discovered thallium-rich parageneses in several sediment-hosted and shear-zone-related gold deposits, such as: (i) Carlin (Nevada, USA) with four new thallium minerals – carlinite (Radtke – Dickson 1975), christite (Radtke et al. 1977), weissbergite (Dickson – Radtke 1978) and ellisite (Dickson et al. 1979); (ii) Mercur (Utah, USA) with two new thallium compounds - gillulyite (Wilson et al. 1991) and fengite (Wilson et al. 1993); and (iii) Hemlo (Ontario, Canada) where a mineralogical study by Harris (1986) revealed an epithermal Tl-rich mineral association composed of parapierrotite, routhierite and two new minerals – criddleite (Harris et al. 1988) and vaughanite (Harris – Roberts 1989). Criddleite was also reported by Gatellier et al. (1990) from the Viges gold deposit in France.

– mineralized veins cutting alkaline rocks of the Ilímaussaq intrusive complex (Greenland) where Semenov et al. (1967) described chalcothallite and Karup-Møller (1978), rohaite.

– a very uncommon occurrence of Tl-bearing mineral phases in Ni-Fe-Cu-PGE ores of the Norilsk district (Russia), where Kovalenker et al. (1976) described a new mineral thalcusite that was also found at Ilímaussaq (Kovalenker et al. 1978) and where Rudashevskii et al. (1979) discovered a new mineral phase named thalfenisite.

– finally, the base-metal Rajpura-Dariba (Rajasthan, India) deposit, where Basu et al. (1983) described a new thallium mineral, rayite.

This brief review of world-wide Tl-mineral occurrences is far from complete. For example, Tl-bearing phases have also been observed in several base-metal and gold deposits, such as Wiesloch (Germany) and the Rambler mine (USA), but generally in a very small amounts.

Jas Roux deposit

The thallium mineralization of the Jas Roux deposit (Lambert coordinates: x = 915.10, y = 286.80; altitude 2170 m; Orcières sheet of the 1:50,000-scale, geographic map of France) was discovered by BRGM (Bureau de Recherches Géologiques et Minières) during fieldwork for a systematic inventory of mineral deposits and ore showings in the Hautes-Alpes Department (Pierrot et al. 1972), after preliminary archive investigations had revealed that a "copper deposit" had been discovered at Jas Roux in 1822. The locality was sampled in 1969 and mineralogical study revealed a mineralization of stibnite, realgar, barite and an unknown Tl-bearing phase, which was later described as a new mineral named pierrotite (Guillemin et al. 1970). An extensive study of the deposit, carried out from 1970 to 1980, revealed three other new Tl minerals: routhierite, laffittite and chabourneite (Johan et al. 1974, 1981). The thallium mineralization of Jas Roux was the subject of a doctorate thesis (Mantienne 1974). Unfortunately, further sampling is now strictly forbidden because the deposit lies within the protected Pelvoux National Park.

Geological setting

The Jas Roux deposit is contained in Triassic sediments of the Morges syncline that partly cover the tectonic junction between three major tectonic units making up the Pelvoux Massif, i. e. (i) the Ecrins anticline, (ii) the Sirac anticline, and (iii) the Crupillouse orthogneiss and Chaillol series (Vernet 1965). The crystalline basement of the Pelvoux Massif comprises three major lithostratigraphic units (Le Fort – Pecher 1971; Le Fort 1973):

(i) The oldest unit is a volcano-sedimentary series affected by high-grade (HT-LP) metamorphism and intruded by granite (Crupillouse orthogneiss) or mafic complexes (Peyre–Arguet unit). This unit includes the crystalline rocks of the Sirac anticline and the strongly migmatized Pigeonnier gneiss of the Ecrins anticline.

(ii) The middle unit, called "formation de la Lavey" by Le Fort (1973), is exposed in the eastern part of the Ecrins anticline and comprises felsic and mafic volcanic and volcano-sedimentary rocks that underwent high-grade (HT-LP) metamorphism and were strongly migmatized by Hercynian granite. Amphibolites within this unit result from the metamorphism of albitized mafic lava flows and related tuff (Le Fort 1973).

(iii) The youngest unit, exposed at the western rim of the Pelvoux Massif, is a slightly metamorphosed felsic volcanic and volcano-sedimentary series intruded by Hercynian granite (Le Fort 1973).

The Hercynian (Carboniferous) granite that intruded and migmatized these crystalline basement rocks is particularly abundant within the Ecrins anticline, north of the Col du Loup shear zone (Giobernay granite and Bans granite).

The overlying Triassic sedimentary series containing the Jas Roux deposit crops out along an E-W-trending shear zone which Vernet (1965) called "suture du Col du Loup en Valgaudemar". Geological mapping at 1:5,000 scale (Fig. 1) has shown that the tectonic contact between the Triassic deposits and the crystalline rocks of the Ecrins anticline dips at 75°–85° N, and is commonly vertical; later NW-SE faulting divided the Triassic series into several tectonic blocks which, for prospecting purposes, were numbered from 0 to 4 (Fig. 1). The stratification within these tectonic blocks has been greatly influenced by E-W- and NW-SE- trending faults and strikes generally N30°–50° W with a dip varying from 50°– 90° SW. To the west, the Triassic outcrops stop at a major NNE-SSW fault, that also affects the crystalline basement rocks of the Sirac anticline (Fig. 1). The contact between the Triassic and the Sirac anticline is masked by colluvial sediments and morains.

Lithostratigraphic study has shown that the Triassic sequence in blocks 0, 1 and 2 is the same, being repeated by NW-SE-trending en echelon faults, with the following succession from the base up:

1. A detrital unit, about 13 m thick. It comprises poorly sorted sandstone and quartzite at the base, with the sandstone being characterized by subangular quartz grains indicating a short distance of transportation. Rare rutile- and zircon-rich beds containing accessory tourmaline are observed. Towards the top of the unit, the sandstone is gradually replaced by poorly sorted medium-grained arkose with a strong predominance of angular potassium feldspar grains devoid of sericitization. Accessory tourmaline is relatively common.

2. A dolomitic unit, about 8 m thick. It consists of dark-grey and brownish dolomite that begins progressively as dolomitic intercalations within the top of the underlying arkose, that evolve into ~20-cm-thick beds separated by intercalations of siltstone and shale. Intraformational breccias, in places enriched in iron hydroxides, are found in approximately the middle of the series.

3. A limestone and marl unit, 19 m thick. Massive limestone at the base evolves rapidly into marl and marly limestone with a 40–80 % carbonate content. In thin section, the limestone exhibits granulometric sorting with a detrital fraction represented by fine-grained quartz and muscovite. Euhedral crystals of pyrite become common upward and iron hydroxides mark the stratification. Several intercalations of pyrite-rich black shale occur in the upper part of the unit.

4. A massive limestone unit, 24 m thick. The limestone is strongly silicified in the vicinity of an E-W-trending fault zone.

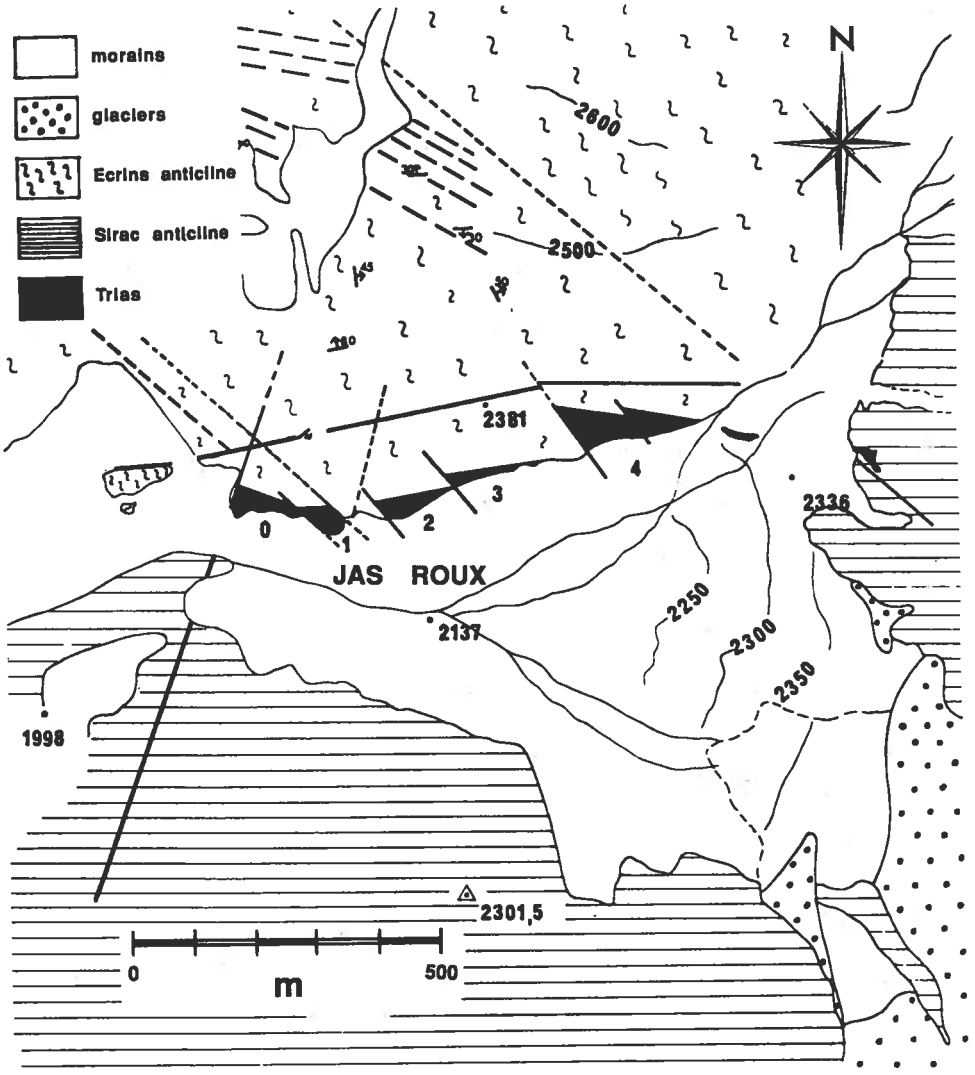

Fig. 1. Simplified geological map of the Jas Roux area showing tectonic blocks of Triassic series (black) numbered form 0 to 4. See text for other explanations.

The Triassic stratigraphy continues in blocks 3 and 4, with:

5. Red-violet calcareous shale, about 2 m thick, including a basic lava flow that has been entirely albitized.

6. Light-grey tuffaceous limestone, 3.5 m thick, with local accumulations of chlorite and euhedral pyrite crystals.

7. Calcareous black shale, about 4 m thick, with, towards the top, dark-grey limestone containing sandstone lenses - a precursor to the subsequent detrital sedimentation.

8. Calcareous sandstone, 12.5 m thick, with intercalated limestone. Predominantly detrital at the base, this unit becomes clayey near the top with the appearance of nodular calcareous shale containing sandstone lenses.

9. Dark-grey to black oolitic limestone, 2 m thick. The oolites have quartz-grain cores and are less than 1 mm in size.

10. Black limestone, about 12 m thick. It forms beds between ~ 5 and 20 cm thick, with black shale intercalations; sandstone lenses are observed in places. This unit marks a transition into a very thick sequence of black shale attributed to the Lias (Vernet 1965).

Mineralization

The Jas Roux Tl-, Hg-, Ag-, As-, Sb-bearing mineralization is best developed in block 2, where it forms a 3.8-m-thick barite-rich zone located between the dolomitic unit (2)[1] and the overlying limestone and marl unit (3). Another, less important, mineralized zone is observed at the contact between unit (3) and the massive limestone unit (4). The mineralization in block 1 is much more diffuse; it occurs throughout the Triassic sequence, with concentrations at the boundaries between the lithological units. Block 0 contains only an insignificant amount of Tl-, As-bearing sulphides despite the fact that barite remains abundant in several beds. Blocks 3 and 4 were not affected by the ore-forming process.

Two sets of joints are observed within the E-W shear zone. The older set, oriented NE-SW with a subvertical dip, hosts the Tl-, Hg-, Ag-, As-, Sb-bearing mineralization. The younger set, oriented NW-SE with a 40°–50° SW dip, is barren.

The hydrothermal ore-forming system began with a pervasive silicification of the Triassic carbonates, giving rise to jasperoid and/or chert composed of randomly

oriented quartz grains, several microns in size. This was a metasomatic process of "grain by grain" replacement of the original carbonate crystals that proceeded along the rock stratification planes and perfectly preserved the original carbonate textures, including the original clay and organic matter impurities, the stratification and the boundaries of small sandstone lenses; we also observed "ghosts" of calcite veins cross-cutting the dolomite.

The chert is cut by quartz veinlets made up of strongly deformed crystals with a stretching oblique to the stratification. Some veinlets are slightly folded, indicating a plastic behaviour of the chert during their formation. This second hydrothermal episode was contemporaneous with the onset of tectonic stresses and is characterized by the precipitation of fluorite and barite. Colorless fluorite {100} crystals are observed exclusively in chert, many of them having been replaced by quartz during later silicification. Barite occurs as veinlets cutting the chert or penetrating it along quartz grain boundaries, and it also metasomatically replaces non-silicified Triassic limestone and dolomite; it was thus clearly later than the silicification. The synkinematic crystallization of barite is obvious from the cataclasis of its crystals and their cementation by fine-grained barite aggregates. Joints filled with adularia and albite (An_8) were observed in hydrothermally altered Triassic dolomite.

Mineralogy of the Jas Roux deposit

Pyrite

Pyrite is ubiquitous in the Jas Roux deposit, and two types can be distinguished: (i) pyrite of synsedimentary origin and (ii) pyrite of hydrothermal origin. The synsedimentary pyrite consists of subhedral crystals forming millimetre-thick beds parallel to the stratification of clay-rich intercalations within the Triassic series. In places, these pyrite-rich beds have been strongly folded and squeezed by tectonic movement. The hydrothermal pyrite, associated with the thallium-bearing mineralization, consists of subhedral or euhedral (pentagon-dodecahedral) crystals interstitial with respect to the host rock. Colloform aggregates of subhedral pyrite crystals are commonly observed. Electron microprobe analyses of the hydrothermal pyrite show a systematic Tl concentration averaging 0.07 wt. % Tl.

Sphalerite

Sphalerite is particularly abundant in block 2 (Fig. 1) where it forms impregnations, associated with lead-sulphosalts, in barite-rich gangue. The sphalerite grains are interstitial to the host-rock minerals, contain abundant mica inclusions in the schistose intercalations and exhibit a strong tendency to euhedral development in the carbonate host rocks. Rare well-developed octahedral crystals have been observed; Graeser (1965) reported this crystal form, resulting from the equilibrium growth of two tetrahedra, for sphalerite in the Lengenbach quarry (Switzerland).

The sphalerite is colorless or slightly honey-yellow, which indicates a low iron content typical of low-temperature parageneses. Electron microprobe analyses show minor concentrations of Fe, Cd and Tl, with the average concentrations (wt. %) being Fe – 0.7, Cd – 0.8, Tl – 0.1.

Phase $Pb_9Ag(Sb,As)_{13}S_{29}$

Polished section study of the Pb-, Sb-sulphosalts has revealed the presence of a mineral phase, associated with twinnite and zinckenite, whose chemical and X-ray data do not correspond to any known mineral species. However, we prefer not to propose a name for this new mineral, because additional chemical and crystallographic data are needed before we can officially describe it.

In polished section, the mineral comprises acicular crystals that form aggregates intimately associated with zinckenite, and are more rarely included in the zinckenite. In reflected light, the crystals are white in air, becoming white-grey in oil. Bireflectance is easily observable in air, giving varied greyish tints. The anisotropy is significantly stronger than that of zinckenite and polarization colours vary from brown to deep-blue, similar to those of jamesonite. Some crystals, investigated in oil, show very thin twin lamellae parallel to the crystal elongation. Very rare internal reflections of a purple-red colour have also been observed in oil. Reflectance measurements (Table 1) show that the reflectivity of this mineral phase is nearly identical to that of jamesonite (Picot – Johan 1983). Micro-indentation hardness measurements gave VHN_{25} = 165 kg/mm² (157–170) for five indentations measured on five different grains.

Qualitative electron microprobe analyses systematically disclosed Pb, Ag, Sb, As, S in major amounts, as well as Tl in some grains. Quantitative electron microprobe analyses (Table 2), calculated on the basis of 52 atoms per formula unit lead to the following empirical formulae:

$$Pb_{9.47}Ag_{0.99}(Sb_{9.52}As_{3.09})_{12.61}S_{28.92},$$
$$(Pb_{9.15}Tl_{0.66})_{9.81}Ag_{1.05}(Sb_{8.00}As_{4.93})_{12.93}S_{28.21}.$$

Consequently, the ideal formula can be written $(Pb,Tl)_9Ag(Sb,As)_{13}S_{29}$. Despite several attempts, we did not succeed in obtaining a fragment suitable for single crystal study. The X-ray powder pattern (Table 3) shows remarkable similarities with the powder pattern of jamesonite, especially for small 2θ diffraction lines. Taking these similarities into account, the X-ray powder pattern was successfully indexed on a monoclinic unit-cell with the following parameters refined by least-squares: a = 17.640(8), b = 18.464(8), c = 3.967(3) Å, β = 90°48', V = 1292 Å³. Z = 1. The calculated density for the composition $Pb_9Ag(Sb_{8.8}As_{4.2})_{13}S_{29}$ with Z = 1 is D_{calc} = 5.51.

[1] The numbers refer to the lithostratigraphic succession described above

Table 1. Reflectances of $Pb_9Ag(Sb,As)_{13}S_{29}$ and jamesonite

	$Pb_9Ag(Sb, As)_{13}S_{29}$		Jamesonite *	
λ (nm)	R_{max} (%)	R_{min} (%)	R_{max} (%)	R_{min} (%)
420	43.7	38.6	41.8	36.6
440	43.2	38.0	41.9	36.5
460	42.5	37.1	41.2	35.6
480	41.9	36.6	41.2	35.3
500	41.4	36.0	40.7	35.1
520	41.1	35.5	40.3	34.6
540	40.4	35.0	39.8	34.0
560	39.7	34.5	39.1	33.5
580	39.3	33.9	38.6	33.1
600	38.4	33.3	38.2	32.9
620	37.8	32.7	37.7	32.4
640	37.0	32.1	37.0	31.8
660	36.2	31.4	36.5	31.6
680	35.2	30.5	35.6	31.1
700	34.5	30.0	35.2	30.8

Measurement conditions: plane polarized light, normal incidence, monochromator, photomultiplier with the S_{20} cathode, standard SiC, objective 44/0.65, half-field prism illuminator. The obliquity was corrected by (R⊥ + R//)/2; * Picot – Johan (1983)

Twinnite

Twinnite occurs in block 2, where it forms local accumulations or millimetre-thick veinlets parallel to the dolomite stratification. Macroscopically, it resembles tetrahedrite, and is commonly associated with the phase $Pb_9Ag(Sb,As)_{13}S_{29}$ whose acicular aspect is also visible macroscopically.

The reflectivity of twinnite (Picot – Johan 1983) is similar to that of other Pb-Sb-, and Pb-As-sulphosalts and thus is difficult to distinguish from these mineral phases in reflected light. Between crossed polars, twinnite shows a strong anisotropy; all crystals are polysynthetically twinned along (100) (Jambor 1967). Micro-indentation hardness measurements gave VHN_{25} = 150 kg/mm² (average of five indentations varying from 145 to 166 kg/mm²); Jambor (1967) indicates VHN_{50} = 147 kg/mm² for twinnite from Madoc (Canada).

Electron microprobe analyses (Table 2) confirm the chemical composition given by Jambor (1967), with the empirical formulae calculated on the basis of 7 atoms being respectively: $Pb_{1.06}(Sb_{1.11}As_{0.86})_{1.97}S_{3.97}$ (analysis 1) and $(Pb_{1.13}Tl_{0.02})_{1.15}(Sb_{0.98}As_{0.89})_{1.87}S_{3.98}$ (analysis 2). It is noteworthy that the $[Sb/As]_{at}$ ratio is close to 1. Similar results were obtained by Jambor (1967) for twinnite from Madoc and by Mozgova et al. (1982) for this mineral phase from the Novoye deposit (Russia).

Our results suggest that the ideal chemical formula of twinnite should be written $PbAsSbS_4$, rather than $Pb(As,Sb)_2S_4$ as given by Jambor (1967). This conclusion is corroborated by the experimental work of Walia – Chang (1973), who studied the ternary PbS-Sb_2S_3-As_2S_3 system and obtained the compound $PbAsSbS_4$ with an extremely narrow stability field. They ascribed this synthetic phase to guettardite (Jambor 1967).

The X-ray powder pattern of the twinnite from Jas Roux was indexed on the following orthorhombic unit-cell refined by least-squares: a = 18.54(1), b = 7.955(3), c = 8.512(3) Å, V = 1323 Å³. Again, these data are nearly identical to those published by Jambor (1967). Weissenberg photographs show a sub-cell with a' = a, b' = b, c' = c/2.

It is to be noted that the X-ray powder pattern of twinnite is nearly identical to that of guettardite (Jambor 1967), and that Bracci et al. (1980) concluded that twinnite and guettardite are dimorphous mineral species. Moreover, Mozgova et al. (1982) reported the structural relationship between these two minerals and sartorite, and proposed to discredit guettardite and to use the name of twinnite for a group of minerals having the general formula $Pb(Sb,As)_{2-x}S_{4-1.5x}$. The existence of this deviation from stoichiometry was obtained by calculating the electron microprobe analyses on the basis of 1 Pb. However, when one takes the crystal chemistry of sulphosalts into account, this approach is hardly acceptable. The electron microprobe analyses of twinnite from Jas Roux, most of the analyses from the Novoye deposit in Russia (Mozgova et al. 1982) and the Hemlo deposit in Canada (Harris 1986), and the analysis of guettardite from the Pitone quarry in Italy (Bracci et al. 1980) show, when calculated on the basis of 4 S, a composition close to the ideal formula $Pb(Sb,As)_2S_4$, with $[Sb/As]_{at}$ ~ 1.

Table 2. Electron microprobe analyses of minerals from the Jas Roux deposit

	1	2	3	4	5	6	7	8	9	10	11	12	13	14
Pb	39.5	42.6	44.0	43.6	32.7	24.6	24.5	–	–	–	–	–	–	–
Tl	n. a.	0.7	n. a.	3.1	–	–	–	21.8	–	–	14.9	12.8	–	–
Ag	–	–	2.4	2.6	–	11.6	11.5	–	44.2	–	–	–	–	44.5
Cu	–	–	–	–	–	–	–	–	–	25.8	–	–	–	–
Hg	–	–	–	–	–	–	–	–	–	28.5	–	–	–	–
Zn	–	–	–	–	–	–	–	–	–	2.1	–	–	–	–
Sb	24.4	21.7	26.0	22.4	39.1	38.6	38.4	39.7	7.6	–	51.4	25.4	12.2	20.7
As	11.6	12.0	5.2	8.5	4.4	2.6	2.5	12.5	21.7	17.4	8.4	29.7	53.1	11.0
S	23.0	23.1	20.8	20.8	23.1	22.3	22.3	25.4	24.7	25.3	26.5	31.5	33.9	23.3
Total	98.5	100.1	98.4	101.0	99.6	99.7	99.2	91.4	98.2	99.1	101.2	99.4	99.2	99.5

Analytical conditions: CAMECA electron microprobe, C. Gilles analyst, 20 kV, 10 nA, standards:
$TlAsS_2$ (for Tl,As), PbS (for Pb), Sb_2S_3 (for Sb), HgS (for Hg), FeS_2 (for S), Ag, Cu, Zn metals; ZAF correction programme; n. a. = not analyzed.
Analyses: 1, 2–twinnite; 3, 4–phase $Pb_9Ag(Sb,As)_{13}S_{29}$; 5–zinckenite; 6, 7–andorite; 8–parapierrotite; 9–smithite; 10–aktashite; 11–$Tl(Sb,As)_7S_{11}$; 12–$Tl(As,Sb)_{10}S_{16}$; 13–wakabayashilite; 14–phase Ag_2SbAsS_4.

Table 3. X-ray powder pattern of $Pb_9Ag(Sb,As)_{13}S_{29}$

I	d_{meas} (Å)	d_{calc} (Å)	hkl
1	4.42	4.41	400
5	4.09	4.09	240
5	3.877	3.877	011
3 d	3.598	3.615	150
		3.586	430
10	3.406	3.406	250
3	3.326	3.333	031
5	3.215	3.217	311
3 d	3.105	3.128	350
3 d	3.049	3.060	530
8	2.960	2.960	141
3	2.901	2.905	260
		2.904	610
7	2.821	2.827	421
7	2.730	2.727	360
4	2.647	2.653	630
1	2.543	2.551	550
3	2.453	2.447	351
3	2.369	2.377	$\bar{6}01$
5	2.288	2.289	180
2	2.221	2.218	$\bar{6}31$
3	2.160	2.155	551
8	2.089	2.091	641
1 d	1.981	1.983	002
		1.981	181
1 d	1.943	1.943	281
1	1.910	1.905	811
6	1.866	1.867	930
		1.866	661
		1.865	312
2	1.814	1.815	$\bar{6}80$
		1.815	142
		1.814	$\bar{1}91$
4	1.783	1.782	291
		1.780	242
3	1.723	1.727	432
3	1.703	1.702	780

Cu/Ni, 240 mm circumference camera, intensities estimated visually from 1 to 10; d = diffuse

The relationship between unit-cells of twinnite and guettardite can be examined in the <a,c> plane of the twinnite structure: $a_{guett} = [a_{tw} + (c/2)_{tw}]/\sin b_{guett}$, $b_{guett} = b_{tw}$, $c_{guett} = c_{tw}/\sin b_{guett}$, $b_{guett} = 90° + \arcsin[(c/2_{tw}/a_{tw})]$. Using these equations and the unit-cell parameters for twinnite from Jas Roux (see above), we obtain the following calculated unit-cell for guettardite: a = 20.47, b = 7.95, c = 8.71 Å, β = 102°05', which has to be compared with the data of Jambor (1967): a = 20.0, b = 7.94, c = 8.72 Å, β = 101°35'. The solution to the relationship between guettardite and twinnite depends on their crystal structure determinations. We suggest that the different symmetry of the unit-cells might be due essentially to a different stacking of Sb and As atoms.

Zinckenite

Zinckenite is the most abundant Pb-sulphosalt within block 2, being everywhere associated with the phase $Pb_9Ag(Sb,As)_{13}S_{29}$ and stibnite, and in places with andorite. It exhibits abundant purple-red internal reflections, which are less common in As-poor zinckenite. Furthermore, it is polysynthetically twinned, with "parquet-like" twins on sections perpendicular to [0001], which is a rather uncommon feature for zinckenite. Micro-indentation hardness measurements gave VHN_{25} = 141 (135–146) kg/mm². Reflectivity values for zinckenite from Jas Roux are systematically lower than those measured for zinckenite from Malé Železné in Slovakia (Picot – Johan 1983), which is poor in arsenic (Table 4), but the intensity of bireflectance is similar in both cases.

Electron microprobe analysis (Table 2) leads to the following empirical formula calculated on the basis of 47 atoms: $(Pb_{5.88}Ag_{0.10})_{5.98}(Sb_{11.97}As_{2.19})_{14.16}S_{26.86}$. This is close to the ideal composition $Pb_6(Sb,As)_{14}S_{27}$. According to Walia – Chang (1973), the As-rich limit of the zinckenite stability field corresponds to the composition $Pb_6(Sb_{9.8}As_{4.2})_{14}S_{27}$. Consequently, the As concentration in zinckenite from Jas Roux corresponds to about 50 mol. % of the As-rich end-member defined by Walia – Chang (1973). It is interesting to note that the high As concentration in zinckenite is restricted to mineral parageneses that are strongly enriched in As, as at Madoc (Jambor 1967) and also at the Hemlo deposit (Harris 1989) where zinckenite contains up to 11.5 wt. % As.

The unit-cell parameters refined by least-squares from the X-ray powder pattern are: a = 44.11(3); c = 8.625(2) Å. Taking into account the data of Jambor (1967) and Walia and Chang (1973), a slight decrease in the c-parameter with As concentration has to be noted.

Andorite

Andorite is the latest Pb-sulphosalt at Jas Roux, crystallizing just before stibnite. It occurs in microscopic aggregates and is intimately associated with the phase $Pb_9Ag(Sb,As)_{13}S_{29}$ and zinckenite. In polished section, andorite fills interstices between zinckenite grains, which makes it difficult to study. Most of the andorite grains are twinned, with triangular-shaped twins being fairly common. Micro-indentation hardness measurements gave VHN_{25} = 162 (153–174) kg/mm².

Table 4. Reflectances of zinckenite

	Jas Roux		Malé Železné*	
λ (nm)	Rmax (%)	Rmin (%)	Rmax (%)	Rmin (%)
420	43.4	37.9	44.4	39.2
440	42.7	38.1	44.6	39.4
460	42.3	37.9	44.5	39.2
480	41.6	37.4	44.2	39.0
500	41.2	37.2	43.8	38.8
520	40.8	36.9	43.2	38.4
540	40.1	36.5	42.5	37.9
560	39.6	36.2	41.8	37.4
580	38.9	35.6	41.0	36.6
600	38.3	35.1	40.4	36.0
620	37.5	34.6	39.8	35.4
640	36.8	33.9	39.0	34.6
660	36.0	33.2	38.2	34.0
680	35.1	32.5	37.3	33.2
700	34.3	31.7	36.2	32.4

* Picot – Johan (1983); for measurement conditions, see Table 1

Electron microprobe analyses (Table 2) confirm the ideal formula $PbAgSb_3S_6$. The average composition corresponds to an empirical formula $Pb_{1.02}Ag_{0.93}(Sb_{2.74}As_{0.29})_{3.03}S_{6.02}$, indicating 9.6% of the Sb-site occupied by As.

The studied material did not allow single crystal examination. Unit-cell parameters refined from the X-ray powder pattern are: a = 12.778(6); b = 19.244(8); c = 4.248(3) Å. These values are significantly lower than those given by Nuffield (1945) for andorite from Bolivia (a = 12.98; b = 19.15; c = 4.26 Å), which can be explained by the presence of As in the andorite from Jas Roux.

Stibnite

Stibnite at Jas Roux forms a mineralized layer about 30 cm thick within block 1, where it is associated with pyrite and sphalerite. Polished section study shows that it is interstitial to the other metallic phases and rock-forming minerals and thus represents a late crystallization. The stibnite aggregates commonly exhibit pressure twins.

In block 2, stibnite is associated either with Pb-sulphosalts or with Tl-bearing minerals and realgar. Where realgar is well developed in joints cutting carbonate rocks, it can contain subhedral stibnite crystals up to 1 cm in length. Rare myrmekitic intergrowths of stibnite and realgar have been observed.

The chemical composition of the stibnite associated with Tl-bearing minerals and realgar was investigated by electron microprobe. No thallium concentration was detected, but analyses systematically showed an average As concentration of 2.6 wt. %. Harris (1986) reported up to 4.8 wt. % As in stibnite from the Hemlo gold deposit.

Chabourneite

Chabourneite was described as a new mineral from the Jas Roux deposit by Johan et al. (1981). It is the most abundant Tl-bearing mineral phase in this deposit, forming black conchoidal aggregates (up to several centimetres in size) associated systematically with realgar, commonly with stibnite and rarely with smithite, routhierite, laffittite and wakabayashilite.

For optical data we refer to the publication by Johan et al. (1981), who also determined a triclinic unit-cell, space group P1, with a = 16.346(5), b = 42.602(10), c = 8.534(3) Å, α = 95.86°(3), β = 86.91°(3), γ = 96.88°(3), V = 5863.5 Å^3. These values can be compared with those given by Nagl (1979), using the transformation matrix /100/0$\bar{1}$0/001/. A sub-structure, with a' = a/2, b' = b/2, c' = c/2, α' = α, β' = β, γ' = γ is obvious from Weissenberg photographs; this was also observed by Nagl (1979).

More than 100 microprobe analyses were carried out on chabourneite from Jas Roux (Johan et al. 1981). They show a partial replacement of Tl by Pb, according to the substitution mechanism $Tl^+ + (Sb,As)^{3+} \rightarrow 2Pb^{2+}$. For the Tl end-member, the average composition calculated on the basis of 1S is $Tl_{0.1430}Sb_{0.3325}As_{0.2872}S$ (Johan et al. 1981). This leads to the empirical formula $Tl_{3.003}(Sb_{6.982}As_{6.031})_{13.013}S_{21}$, or ideally $Tl_3(Sb_7As_6)_{13}S_{21}$. The calculated density for this composition and Z = 7 is D_{calc} = 5.13, in perfect agreement with D_{meas} = 5.10 (Johan et al. 1981). According to this substitution mechanism, the chemical formula of the Pb end-member should be written $Pb_6(Sb,As)_{10}S_{21}$. On the basis of their study of the Pb-Sb-S system, Craig et al. (1973), proposed this formula for robinsonite. However, Jambor – Plant (1975) performed an extensive electron microprobe study of natural robinsonite samples and concluded that the theoretical formula of robinsonite may be $Pb_4Sb_6S_{13}$.

Nagl (1979) studied a Pb-rich chabourneite from Jas Roux and proposed the formula $Tl_8Pb_4Sb_{21}As_{19}S_{68}$ for which he determined the crystal structure. However, he did not take into consideration the existence of a pure Tl end-member and the possibility of Tl replacement by Pb. The average composition of the chabourneite studied by Nagl (1979) corresponds to the formula $Tl_{2.31}Pb_{1.18}(Sb_{6.71}As_{5.56})_{12.27}S_{21}$. Compared to the composition of the Tl end-member, $Tl_3(Sb_7As_6)_{13}S_{21}$, this shows a deficit in the Tl and (Sb,As) sites of 0.69 and 0.73 atoms respectively, and confirms the substitution mechanism indicated above. Furthermore, it must be stressed that the calculated density (D_{calc}) of 4.88 given by Nagl (1979) for the above formula is significantly lower than the measured value (D_{meas}) of 5.10, published by Johan et al. (1981).

In conclusion, the existing data on chabourneite reveal a number of discrepancies, especially concerning its chemical formula and crystal structure. The study of this mineral species needs to be reviewed and completed.

Parapierrotite

Parapierrotite was described as a new mineral by Johan et al. (1975) from Allchar in Macedonia. It was discovered at Jas Roux at approximately the same time, where it occurs as rare microscopic grains and aggregates included in realgar within the block 1. Harris (1986) has also described parapierrotite from the Hemlo gold deposit.

Examination of the Jas Roux parapierrotite in reflected light shows that sections perpendicular to (010) are nearly isotropic. This behaviour makes it possible, in polished section, to distinguish parapierrotite from pierrotite and chabourneite, which remain anisotropic at any crystallographic orientation. Internal purple-red reflections are rare in air, but frequent in oil. The micro-indentation hardness measured on a nearly isotropic grain was VHN_{25} = 134 kg/mm^2 (128–142 kg/mm^2), which is significantly higher than 76 kg/mm^2 measured for parapierrotite from Allchar (Johan et al. 1975).

Electron microprobe analysis (Table 2) leads to the following empirical formula calculated on the basis of 14 atoms: $Tl_{1.07}(Sb_{3.28}As_{1.68})_{4.96}S_{7.97}$. This shows 34 % oc-

cupation of the Sb-site by As, which again is higher than for parapierrotite from Allchar (12.6 % of the Sb-site occupation by As; Johan et al. 1975). X-ray study confirmed the results published by Johan et al. (1975). The crystal structure of parapierrotite was determined on a synthetic material by Engel (1980), after Edenharter – Peters (1979) had succeeded in a hydrothermal synthesis of the mineral from aqueous solutions at 200 °C.

Pierrotite

Pierrotite, described as a new mineral from the Jas Roux deposit by Guillemin et al. (1970), is mainly associated with chabourneite and parapierrotite. In reflected light, it has a stronger anisotropy and less abundant purple-red internal reflections than chabourneite. Other optical data are given in the publication of Guillemin et al. (1970).

The formula of pierrotite was given by Guillemin et al. (1970) as $Tl_2(Sb,As)_{10}S_{17}$, but Engel et al. (1983) in determining the crystal structure redefined the formula as $Tl_2Sb_6As_4S_{16}$. This composition is more probable, because of the electroneutrality of the formula, considering Tl^{1+}, Sb^{3+}, As^{3+} and S^{2-}. The analysis given by Guillemin et al. (1970) and recalculated on the basis of 16 S, leads to $Tl_{1.89}(Sb_{7.17}As_{2.28})_{9.45}S_{16}$, which can be ideally written as $Tl_2(Sb,As)_{10}S_{16}$. However, the $[Sb/As]_{at}$ ratio is far from that used for the crystal structure determination by Engel et al. (1983).

Smithite

Smithite is an extremely rare mineral that was discovered at Lengenbach (Solly 1905) and whose chemical composition was established by Smith – Prior (1907). More recent studies of the smithite from Lengenbach were made by Nowacki – Bahezre (1963) and Graeser (1965). Seeliger (1954) reported a mineral associated with hutchinsonite and tentatively determined as smithite from the Wiesloch deposit in Germany.

The smithite at Jas Roux is the second confirmed occurrence of this mineral in the world (Johan – Pierrot 1971). It is the most abundant silver-bearing mineral phase of the deposit and forms subhedral crystals reaching a maximum of about 1 cm in size with a perfect cleavage.

In reflected light, smithite is white with a bluish tint. In oil, it becomes blue-white compared to pierrotite and chabourneite. Cleavage traces along (100) are always visible and constitute an important determination criterion. The mineral shows a very weak bireflectance in both air and oil, and has a weak anisotropy (comparable to that of lorandite and weaker than that of cinnabar) hidden by abundant purple- red internal reflections. The reflectivity of smithite (Table 5) is close to the reflectivities of proustite and pyrargyrite. The micro-indentation hardness measurements gave VHN_{25} = 53 kg/mm² (average of five measurements).

Electron microprobe analysis (Table 2) revealed a significant replacement of As by Sb, which reflects high antimony activity in the mineralization episodes preceding the precipitation of smithite. The chemical formula calculated on the basis of 4 atoms is $Ag_{1.07}(As_{0.76}Sb_{0.16})_{0.92}S_{2.01}$, and the X-ray powder pattern was indexed with the following parameters: a = 17.23(6); b = 7.781(3); c = 15.196(6) Å, β = 101.2°; Z = 24; D_{calc} = 5.08.

Laffittite

Laffittite, a new mineral described by Johan et al. (1974) from the Jas Roux deposit occurs associated with routhierite and, more rarely, with realgar and Sb-Tl-sulphosalts. Johan et al. (1974), in addition to describing its physical, optical and chemical data, found a monoclinic unit-cell, $P2_1/c$, with the following parameters: a = 6.567; b = 14.02; c = 6.388 Å; β = 119.1°. However, these data were obtained on a poor-quality chip scraped from the polished section. Nakai – Appleman (1983), who studied laffittite from the Getchell mine in Nevada (USA), also concluded that it has a monoclinic unit-cell, but with space group A2/a, and a = 7.732(3); b = 11.285(7); c = 6.643(4) Å; β = 115.16(3)°. They produced a synthesis of this compound and determined its crystal structure, which shows a close relationship to marrite, $PbAgAsS_3$.

Routhierite

Routhierite is another new mineral described by Johan et al. (1974) from the Jas Roux deposit; later, it was found in the Hemlo gold deposit (Harris 1986). Johan et al. (1974) published microprobe analyses leading to empirical formulae of:

$(Tl_{0.495}Cu_{0.304}Ag_{0.175})_{0.974}(Hg_{0.859}Zn_{0.152})_{1.011}(As_{0.875}Sb_{0.106})_{0.981}S_{3.034}$,
$(Tl_{0.478}Cu_{0.296}Ag_{0.193})_{0.967}(Hg_{0.850}Zn_{0.159})_{1.009}(As_{0.874}Sb_{0.116})_{0.990}S_{3.032}$.

They concluded that the ideal formula of routhierite should be written (Tl,Cu,Ag)(Hg,Zn)(As,Sb)S_3. However, if we consider the general formula in the form of

Table 5. Reflectances of smithite

	Grain 1		Grain 2	
λ (mn)	R_{max} (%)	R_{min} (%)	R_{max} (%)	R_{min} (%)
420	43.4	42.0	41.4	40.0
440	42.4	40.7	40.3	39.2
460	41.4	39.6	39.4	38.6
480	40.4	38.9	38.6	37.8
500	39.2	38.0	37.7	37.0
520	38.0	37.0	36.6	36.0
540	36.6	35.8	35.5	35.0
560	35.4	34.6	34.5	33.8
580	34.6	33.6	33.4	32.7
600	34.0	32.8	32.6	31.7
620	33.5	32.2	32.0	31.1
640	33.0	31.6	31.4	30.8
660	32.4	31.2	31.0	30.7
680	31.8	30.8	30.5	30.2
700	31.1	30.6	30.0	29.8

for measurement conditions, see Table 1

$ABCS_3$, where A = Tl, Cu, Ag; B = Hg, Zn; C = Sb, As, we note that the A sites are occupied by monovalent elements with different ion-radii (in Å): Tl^+ (1.47), Cu^+ (0.96), Ag^+ (1.26) (Shannon – Prewitt 1970). Furthermore, the average empirical formula, taking into account the data given above, is $Tl_{0.5}(Cu,Ag)_{0.5}(Hg,Zn)(As,Sb)S_3$. This indicates different sites in the routhierite crystal structure for Tl on one side and Cu and Ag on the other side. Consequently, the ideal formula of routhierite must be written $Tl(Cu,Ag)(Hg,Zn)_2(As,Sb)_2S_6$. Harris (1986) came to the same conclusion for routhierite from the Hemlo gold deposit.

X-ray single crystal study showed routhierite to be tetragonal with a = 9.977(2); c = 11.290(3) Å, Z = 4, D_{calc} = 5.83 for the average chemical composition indicated above (Johan et al. 1974). Graeser (1988) described a new mineral named stalderite, $TlCu(Zn,Fe,Hg)_2As_2S_6$, from the Lengenbach deposit; it is isostructural with routhierite (a = 9.865; c = 10.938 Å) and represents the Zn end-member of this complex solid solution series.

Aktashite

Two anhedral crystals of aktashite, ~0.5 mm in size and included in realgar, were observed at Jas Roux. Under the binocular they are brownish-black and show a high metallic luster. No cleavage is observed. In polished section, aktashite resembles a tetrahedrite-group mineral, being white with a well pronounced creamy tint. Its reflectivity (Table 6) is close to that of tennantite. Reflectivity measurements indicate an extremely weak bireflectance, lying within the measurement error range. The anisotropy is very weak with brownish-grey to blue-grey colours. Micro-indentation hardness measurements gave VHN_{50} = 304 kg/mm² (average of five measurements varying from 302 to 311 kg/mm²).

An X-ray single crystal study by Weissenberg camera gave a rhombohedral unit-cell with the following parameters refined by least-squares from the powder pattern (Table 7): a = 8.484(2) Å; α = 107°24', or respectively a_{hex} = 13.676(4); c_{hex} = 9.314(2) Å. These data are nearly identical to those of Gruzdev et al. (1972). The Weissenberg patterns reflect a sphalerite-type cubic super-structure with a = 5.372(2) Å. Kaplunnik et al. (1980) determined the crystal structure of aktashite, leading to the ideal formula $Cu_6Hg_3As_4S_{12}$ and invalidating the formula $Cu_6Hg_3As_5S_{12}$ given by Gruzdev et al. (1972). Nowacki (1982) discovered an isostructural relationship between aktashite and nowackiite, $Cu_6Zn_3As_4S_{12}$. Furthermore, aktashite forms a solid solution with gruzdevite, $Cu_6Hg_3Sb_4S_{12}$ (Spiridonov et al. 1981). Harris (1986) described aktashite from the Hemlo deposit as showing a significant solid solution with gruzdevite.

Electron microprobe analysis (Table 2) leads to the following empirical formula calculated on the basis of 12 S: $Cu_{6.17}(Hg_{2.16}Zn_{0.49})_{2.65}As_{3.53}S_{12}$. This implies that aktashite from the Jas Roux deposit contains 18.5 mol. % of nowackiite in solid solution, and shows important deviations from the ideal composition. A similar feature was observed by Marumo – Burri (1965) for nowackiite.

Table 6. Reflectances of aktashite

	Grain 1		Grain 2	
λ (mn)	R_{max} (%)	R_{min} (%)	R_{max} (%)	R_{min} (%)
420	29.2	30.4	29.5	30.3
440	30.6	31.0	30.8	31.1
460	30.5	30.8	30.6	30.8
480	30.4	30.5	30.5	30.5
500	30.3	30.2	30.5	30.2
520	30.3	30.0	30.6	30.0
540	30.1	29.8	30.3	29.8
560	29.9	29.5	30.1	29.5
580	29.7	29.3	30.0	29.3
600	29.5	29.0	29.8	29.0
620	29.3	28.8	29.6	28.8
640	29.1	28.6	29.4	28.5
660	28.9	28.3	29.2	28.3
680	28.7	28.1	29.0	28.1
700	28.5	27.8	28.8	27.8

for measurement conditions, see Table 1

Wakabayashilite

Wakabayashilite at Jas Roux is associated with smithite and stibnite in veinlets several centimetres thick. It forms

Table 7. X-ray powder pattern of aktashite

I	d_{meas} (Å)	d_{calc} (Å)	hk.l
4	6.835	6.835	11.0
5	5.006	5.000	02.1
2	4.333	4.335	01.2
4	4.048	4.035	21.1
2	3.666	3.662	20.2
10	3.104	3.104	00.3
		3.098	13.1
3	2.827	2.826	11.3
		2.822	40.1
7	2.685	2.684	31.2
4	2.592	2.608	32.1
		2.584	41.0
1	2.448	2.440	30.3
5	2.293	2.298	22.3
		2.295	05.1
4	2.070	2.073	51.1
		2.067	21.4
4	1.986	1.986	41.3
9	1.900	1.901	13.4
1	1.666	1.665	06.3
		1.664	70.1
8	1.620	1.621	31.5
		1.617	62.1
2	1.572	1.571	51.4
6	1.550	1.554	00.6
		1.549	26.2
1	1.498	1.497	44.3
		1.496	54.1
6	1.342	1.342	62.4
7	1.232	1.232	26.5
		1.232	65.1; 19.1
5	1.202	1.202	25.6

Cu/Ni, 240 mm circumference camera, intensities estimated visually from 1 to 10

yellow-orange fibrous aggregates with fibres oriented perpendicularly to the veinlet walls. In reflected light, it is bluish-grey with a brownish tint in oil. Bireflectance is very weak in sections parallel to [001] and non-existant in the section perpendicular to [001]. The anisotropy is weak, hidden by massive yellow internal reflections. The micro-indentation hardness measured on sections parallel to [001] was VHN_{25} = 70 kg/mm². Reflectivity measurements carried out on sections parallel to [001] show (Table 8) that the reflectivity of wakabayashilite is close to that of orpiment.

Kato et al. (1970) attributed wakabayashilite with the chemical formula $(As,Sb)_{11}S_{18}$ and a pseudo-hexagonal, monoclinic unit-cell having a = 25.17, b = 6.48, c = 25.24 Å, β = 120°00'; V = 3565.15 Å³, Z = 6, D_{calc} = 4.09. Scott – Nowacki (1975) reported a pseudo-hexagonal, monoclinic super-cell with a = 29.128, b = 6.480, c = 29.128 Å, β = 120°, Z = 8 $[(As,Sb)_{11}S_{18}]$. They suggested the ideal formula $Sb_2As_{20}S_{36}$ with Z = 4.

The average chemical composition of wakabayashilite from the Jas Roux deposit, based on five electron microprobe analyses carried out on various fibrous crystals (Table 2), is remarkably different from analytical data published by Kato et al. (1970), especially as far as the S concentration is concerned. This result leads to an emipirical formula that is much simpler than the one proposed by Kato et al. (1970). Calculated on the basis of 7 atoms, the empirical formula of wakabayashilite from Jas Roux is $(As_{2.659}Sb_{0.376})_{3.035}S_{3.965}$, or ideally $(As,Sb)_3S_4$.

The X-ray powder pattern of wakabayashilite from Jas Roux was succesfully indexed on a pseudo-hexagonal unit-cell with a = 25.252(5), c = 6.481(2) Å, V = 3579 Å³ (Table 9). However, the weak line with d = 4.027 Å (Table 9) could not be indexed. According to Scott – Nowacki (1975) it corresponds to the monoclinic super-cell (hkl = $\bar{7}02$). For Z = 24 and the empirical formula indicated above, the calculated density is D_{calc} = 4.14, which is in a good agreement with the measured density D_{meas} = 3.96, of Kato et al. (1970).

Table 8. Reflectances of wakabayashilite and $Tl(Sb,As)_7S_{11}$

	wakabayashilite		$Tl(Sb, As)_7S_{11}$
λ (nm)	Rmax (%)	Rmin (%)	Rm (%)
420	30.0	26.6	28.9
440	28.0	26.5	31.3
460	26.7	25.4	32.1
480	25.1	23.7	31.7
500	24.0	22.8	31.0
520	23.3	21.9	30.3
540	22.7	21.2	29.5
560	22.2	20.8	28.7
580	22.1	20.5	27.9
600	21.9	20.4	27.3
620	21.8	20.4	26.8
640	21.6	20.2	26.4
660	21.8	20.4	26.6
680	21.6	20.5	27.1
700	22.0	20.5	27.6

measurement conditions, see Table 1; Rm = average reflectance

All these data show that wakabayashilite needs to be reviewed, and that the determination of its crystal structure is essential for the definition of its chemical formula.

Phase $Tl(As,Sb)_{10}S_{16}$

Guillemin et al. (1970) reported the occurrence of an amorphous Tl-bearing mineral associated with pierrotite and stibnite and whose composition, according to electron microprobe analyses, corresponds to the empirical formula $Tl_{1.03}(As_{6.45}\ Sb_{3.42})_{9.87}S_{16.10}$. This mineral phase, which at the beginning of the study of the Jas Roux deposit appeared to be rather abundant, was in fact observed only in type-samples of pierrotite studied by Guillemin et al. (1970).

It is interesting to note that the mineral is characterized by a predominance of As over Sb. An experimental study performed on the system Tl-As-Sb-S (unpublished data of C. Maurel) showed that the Sb-rich phases belonging to this system crystallize easily, whereas the As-rich phases remain amorphous under the same experimental conditions.

Table 9. X-ray powder pattern of wakabayashilite

I	dmeas (Å)	dcalc (Å)	hk.l
2	12.6	12.6	11.0
10	6.31	6.312	22.0
7	5.756	5.763	11.1
7	4.774	4.772	41.0
2	4.480	4.522	22.1
1	4.219	4.208	33.0
1	4.027		
6	3.847	3.844	41.1
10	3.500	3.500	52.0
8	3.242	3.241	00.2
3	3.153	3.156	44.0
7	3.081	3.080	52.1
3	2.891	2.896	71.0
2	2.834	2.838	44.1
4	2.757	2.755	63.0
1	2.639	2.644	71.1
4	2.567	2.567	33.2
5	3.533	2.535	63.1
		2.525	55.0
7	2.429	2.430	90.0
		2.422	60.2
5	2.239	2.239	82.1
5	2,138	2.140	74.1
2	2.070	2.071	10.1.0
3	2.024	2.022	30.3
3	1.925	1.925	93.0
		1.922	33.3
		1.921	82.2
6	1.846	1.846	85.1
2	1.821	1.822	12.0.0
2	1.737	1.738	77.1; 11.2.1
2	1.703	1.700	63.3
4	1.670	1.672	96.0
3	1.619	1.620	00.4
		1.619	96.1
8	1.590	1.590	12.3.0

Cu/Ni, 240 mm circumference camera, intensities estimated visually from 1 to 10

Phase $Tl(Sb,As)_7S_{11}$

This Tl-bearing phase occurs as veinlets, less than 30 microns thick, cross-cutting realgar, and consequently is one of the last crystallized mineral phases within the Jas Roux mineralization. The fact that this phase has nowhere been observed outside of realgar suggests a genetic relationship between the two minerals.

The reflectivity is distinctly higher than that of realgar, being slightly lower than the minimal reflectivity of chabourneite (Table 8). Between crossed polars, the mineral shows pervasive red internal reflections. Its anisotropy is weak, but always observable, with bluish polarization colours. Optical properties indicate a crystalline nature of this Tl-bearing mineral phase. However, due to the minuteness of veinlets, we did not succeed in obtaining its X-ray powder pattern. Electron microprobe analysis (Table 2) corresponds to an empirical formula of $Tl_{0.97}(Sb_{5.60}As_{1.48})_{7.08}S_{10.95}$, or ideally to $Tl(Sb,As)_7S_{11}$.

Phase Ag_2SbAsS_4

This mineral phase results from a reaction between smithite and routhierite and forms a myrmekitic intergrowth with routhierite at the contact with smithite. In polished section it resembles stibnite. However, despite a strong anisotropy, the polarization colours are less than for stibnite, ranging from deep grey to bluish-white. The mineral shows a strong bireflectance, from white to grey in air. No internal reflections were observed, even in oil. The reflectivity is close to that of stibnite.

Electron microprobe analysis (Table 2) leads to the following empirical formula calculated on the basis of 4 atoms: $Ag_{1.13}(Sb_{0.47}As_{0.40})_{0.87}S_{2.00}$. This composition is close to a mineral phase located in the middle of the $AgSbS_2 - AgAsS_2$ series.

However, the end-members of this series – miargyrite ($AgSbS_2$), smithite and trechmannite ($AgAsS_2$) – are not isostructural, and thus not highly miscible amongst themselves. This is clearly apparent when one considers the chemical composition of smithite from Jas Roux (see above). Furthermore, the optical properties of this mineral are strikely different from those characterizing the mineral phases indicated above. Unfortunately, the grain size of this interesting mineral observed in polished section did not allow us to obtain its X-ray powder pattern.

Taking into account the crystal chemistry of mineral phases belonging to the $AgSbS_2 - AgAsS_2$ system, we believe that the ideal formula of this phase must be written Ag_2SbAsS_4.

Realgar

Realgar is one of the most abundant ore minerals in the Jas Roux deposit. It forms local accumulations, being commonly associated with stibnite and Tl-bearing minerals. Locally, it fills fissures in the host rock. Electron microprobe analyses did not reveal Tl and Hg concentrations, but systematically showed a low Sb content of, on average, 0.6 wt. % Sb. Similar Sb concentrations in realgar were reported by Harris (1986) from the Hemlo deposit.

Other minerals

Orpiment was observed, although rarely, associated with realgar and Tl-bearing minerals. Unlike wakabayashilite, which forms fibrous crystals, orpiment occurs as lamellar aggregates. *Valentinite* forms hemispherical radial-fibrous aggregates, one to two millimetres in size, occurring in joints of the host rock near the mineralization. The alteration of pyrite gives rise to *gypsum* and *goethite*. Pierrot et al. (1972) reported the occurrence of *kermesite* and *pharmacosiderite*.

Discussion

The crystallization sequence of the Jas Roux mineralization is given in Figure 2. Pyrite was the first sulphide to crystallize from the ore-forming hydrothermal fluid. Its strong tendency to precipitate as colloform aggregates and its rather high Tl-content reflect an epithermal origin. Furthermore, its high Tl concentration indicates the presence of thallium in the fluid from the earliest mineralization stages.

The low Fe concentration in sphalerite, which precipitated after pyrite during the initial mineralization episode, is due to a high sulphur fugacity (pyrite stability field) in the ore-forming system. The significant Cd concentration is characteristic of a low-temperature origin.

The next mineralization episode comprised lead sulphosalts that crystallized in the following order: twinnite, the phase $Pb_9Ag(Sb,As)_{13}S_{29}$, zinckenite and andorite. This episode ended with the crystallization of stibnite. Except andorite and the phase $Pb_9Ag(Sb,As)_{13}S_{29}$, the minerals all belong to the ternary $PbS-Sb_2S_3-As_2S_3$ system studied by Walia – Chang (1973). Considering a low Ag-content in the phase $Pb_9Ag(Sb,As)_{13}S_{29}$, its composition can be tentatively plotted onto the $PbS-Sb_2S_3-As_2S_3$ plane (Fig. 3). Experimental data by Craig et al. (1973) and Garvin (1973) on the binary $PbS-Sb_2S_3$ system showed a large stability of naturally occurring phases: galena, boulangerite, robinsonite, zinckenite and stibnite. However, these studies raised the problem of the robinsonite chemical formula, which is still unsolved.

Taking into account the chemistry of the mineral phases plotted on Figure 3, it appears that the crystallization sequence of the lead sulphosalts depended essentially on two parameters: the $[Sb/As]_{at}$ ratio and the Pb-concentration in the fluid. Thus, the first mineral to crystallize was twinnite, the most As-rich sulphosalt of this mineralization episode. Rapid As impoverishment of the ore-forming system along with an increase in Pb concentration (see Fig. 3), led to the precipitation of the phase $Pb_9Ag(Sb,As)_{13}S_{29}$, the most Pb-rich sulphosalt of this mineralization episode, and also of the whole Jas Roux mineral-

ization. The fact that the studied mineralization is devoid of galena and boulangerite, indicates high Sb- and As-activity in the ore-forming system with respect to Pb. In addition, the absence of robinsonite confirms the results of Garvin (1973) on the instability of this mineral phase below 300 °C; moreover, Walia – Chang (1973) obtained an extremely narrow stability field for robinsonite (Fig. 3). After crystallization of the phase $Pb_9Ag(Sb,As)_{13}S_{29}$, the ore-forming system became increasingly enriched in Sb, and zinckenite precipitated before the crystallization of stibnite. Note that the chemical composition of the phase $Pb_9Ag(Sb,As)_{13}S_{29}$ indicates a concentration of Ag in the ore-forming fluid, which would have increased after the precipitation of zinckenite due to the fact that Ag cannot be incorporated into the zinckenite crystal structure. Hence the crystallization of andorite.

It is interesting to note that the mineralization episodes described above correspond to the sequence found worldwide in sulphide-bearing deposits: pyrite → sphalerite → galena. In the present case, galena is replaced by the association of Pb-, Sb-, As-sulphosalts formed as a result of high Sb- and As-activity in the ore-forming fluid. Moreover, the lithostratigraphic study showed that the stibnite-rich association occurs not only within the main orebody, but is also located at the top of the lithostratigraphic limestone and marl unit (3).

The mineralization episodes that followed the crystallization of stibnite are characterized by a predominance of As, Tl and Hg. The first of these episodes started with the precipitation of wakabayashilite whose $[Sb/As]_{at}$ is 0.07 (Fig. 2), following by a crystallization sequence that was again controlled by an increasing $[Sb/As]_{at}$ ratio. The Tl-bearing minerals (chabourneite, pierrotite) replaced stibnite along its cleavage plane, with chabourneite crystallizing before pierrotite – polished section study shows that the latter forms rims on chabourneite aggregates and

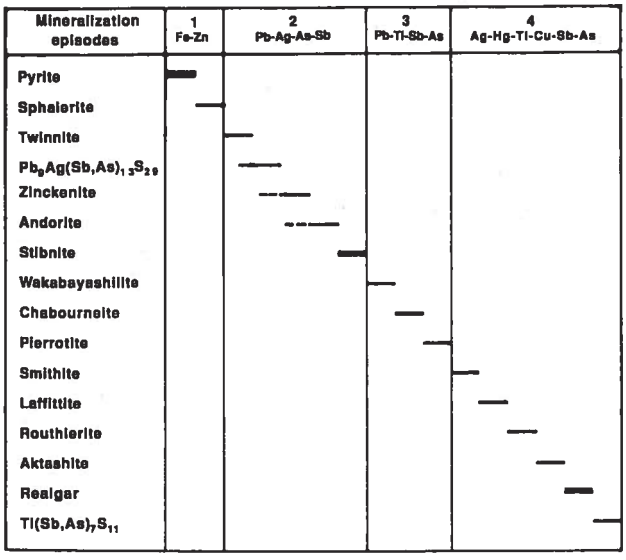

Fig. 2. Crystallization sequence of ore minerals in the Jas Roux deposit.

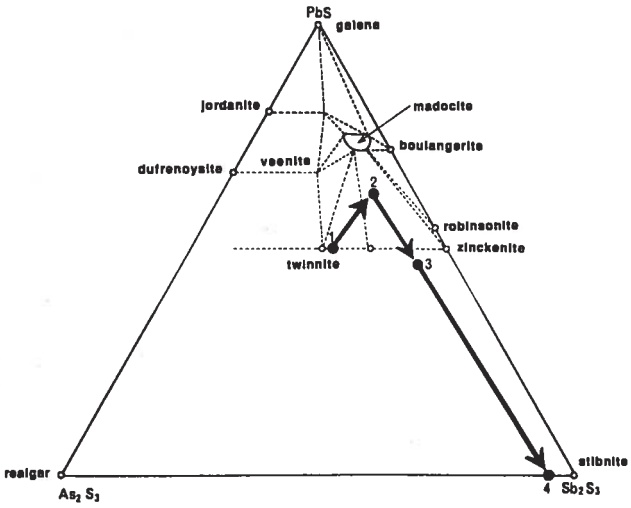

Fig. 3. Phase relations in the system PbS – Sb_2S_3 – As_2S_3 (Walia – Chang 1973) showing compositions of twinnite (1), the phase $Pb_9Ag(Sb,As)_{13}S_{29}$ (2), zinckenite (3) and stibnite (4) from the Jas Roux deposit. Arrows indicate the succession of crystallization.

replaces it along grain boundaries. It is also interesting to note a significant Pb-content in the chabourneite. The position of parapierrotite within the crystallization sequence could not be established due to the rarity of this mineral – we know only that it crystallized before realgar.

The fourth mineralization episode was nearly devoid of Sb, and Tl, Ag and Hg became important. Unlike the mineralization of the previous episodes, which is contained within a well-defined orebody, the minerals of the fourth episode are exclusively disseminated in the Triassic sediments of tectonic block 2, and a strong tendency to metasomatic replacement of earlier crystallized ore minerals is observed in polished section. Furthermore, reactions between the minerals of this fourth episode are also noted. For example, where smithite, the earliest mineral phase of the episode, is replaced by routhierite, a myrmekitic intergrowth with the phase Ag_2AsSbS_4 is seen. The Hg-rich minerals, routhierite and laffittite, precipitated after smithite and replacement of laffittite by routhierite has also been observed. We consider that the mineralization episode ended with the crystallization of aktashite, because this mineral phase contains major Zn and Cu – elements that appear as minor constituents in the routhierite. The abundant metasomatic replacements and reactions among the minerals of the fourth mineralization episode indicate disequilibrium conditions in the ore-forming system at low temperature.

The entire mineralization process at the Jas Roux deposit basically ended with the crystallization of realgar, which is seen to replace all the older minerals, even though a Tl-bearing sulphosalt, later than realgar, occurs locally.

The crystallization sequence of major ore-forming elements in the Jas Roux deposit thus corresponds to Fe → Zn → Pb → Ag → Sb → Tl → Ag → Hg → Cu → Zn → As. When one considers the chemical characteristics of the successive mineralization episodes, it is obvi-

ous that the ore-forming system became enriched in volatile elements: Sb → Tl → Hg → As. Moreover, trace-element analysis has revealed a significant lithium concentration (up to 700 ppm) in the hydrothermally silicified Triassic rocks, which is attributed to Li-rich micas of hydrothermal origin.

Comparison with other Tl-bearing occurrences worldwide, shows several specific metallogenic features of the Jas Roux mineralization. In the Allchar district (Macedonia), Ivanov (1965) reported a metallogenic zoning with an Sb-rich core zone, rimmed by a Tl- and As-rich zone and a strongly silicified and dolomitized outer halo, with all the mineralization being related to andesitic flows and associated tuff. Thus we see several similarities between Allchar and Jas Roux, i. e. (i) a crystallization sequence comprising early Sb-rich and late Tl-rich mineral parageneses, (ii) extensive silicification of the host rock, and (iii) an association with volcanic rocks. Conversely, at Lengenbach (Switzerland), Tl- and Sb-bearing mineral phases are very rare and the paragenesis is dominated by As and Pb; furthermore, there is no extensive hydrothermal alteration of the host rock.

Some sediment-hosted gold deposits containing thallium minerals also exhibit hydrothermal alteration and ore-deposition sequences similar to those observed at Jas Roux. The Carlin deposit (Nevada, USA), for example, is hosted by carbonate rocks of Siluro-Devonian age that are strongly silicified in the vicinity of the orebody. Furthermore, barite is an abundant gangue mineral (Bakken – Einaudi 1986).

The pervasive silicification at Jas Roux implies low-temperature hydrothermal fluids with high silica activity. It is interesting to note that thermal waters within some high-temperature geothermal fields give rise, from time to time, to metal-rich precipitates containing Ag, Hg, Tl, Au, As, Sb. Here, for example, we can cite the Taupo volcanic zone in New-Zealand (Weissberg 1969; Browne – Ellis 1970; Eslinger – Savin 1973), which is associated with recent volcanics (rhyolites and dacites), the Salton Sea brine, California, USA (White 1965, 1968) and the Steamboat springs, Nevada, USA (White 1967; Skinner et al. 1967). In addition to Na, Cl, CO_2 and SiO_2, these hydrothermal brines contain significant concentrations of Li, F and B.

Thermal waters of the Rotokawa geothermal system (Taupo volcanic zone) are depositing muds and silica-rich sinters with high concentrations of above indicated metals (Krupp – Seward 1987). The precipitation of sulphides is related to cooling (Browne – Lloyd 1987), boiling and to the partitioning of dissolved gases (CO_2, H_2S) into the steam phase (Krupp – Seward 1987). Seward – Kerrick (1996) estimated the global hydrothermal CO_2 flux for various hydrothermal systems in the Taupo volcanic zone. They concluded that the CO_2 flux from subareal environment may be comparable to that from volcanic vents.

Within the Taupo hydrothermal system, the ore-depositing fluid is near-neutral pH alkali chloride water. There is no direct information about the mechanism of metal transport. Seward (1973), Krupp – Seward (1987) suggested that gold is transported as thio-complexes and Pb, Zn as a chloride complex (Browne – Lloyd 1987). Ewers – Keays (1977) showed that at Ohaaki, As, Sb, Au and Tl are concentrated near the surface, whereas Zn, Cu, Pb and Te are concentrated in sphalerite, galena, chalcopyrite, argentite, associated with pyrite, marcasite and pyrrhotite, from deeper parts of the reservoir. Sphalerite-hosted fluid inclusions show a broad range of compositions; vapor-rich inclusions coexist with the high-salinity inclusions, indicating that boiling occurred during trapping at about 200–270 °C (Browne – Lovering 1973; Simons – Browne 1997).

The origin of the Jas Roux deposit from low-temperature hydrothermal fluids similar to those observed in active geothermal systems is also indicated by the nature of the hydrothermal alteration, and in particular by the precipitation of cryptocrystalline silica in the form of chert and by the occurrence of adularia, albite, calcite and fluorite in some silicified zones. All these minerals are characteristic of the hydrothermal alteration zone at Broadlands, New-Zealand (Browne 1971, Browne – Lloyd 1987). Skinner et al. (1967) have also reported the presence of fluorite in precipitates from the Salton Sea brine. Furthermore, the Li/K ratios of these brines are rather high (White 1968; Weissberg 1969), which could explain the significant concentration of Li in the alteration zones of mineralization related to this kind of hydrothermal system.

Although the Jas Roux mineralization has not been dated, there is the question of the volcanism capable of generating this ore-forming hydrothermal system. The only volcanic rocks spatially associated with the mineralization are the basic lava flows and tuffs occurring higher in the Triassic series, near the contact with the Lias. However, Vatin-Perignon et al. (1972) reported the presence of rhyolite within the "linéament de la Pilatte", about 3 km NE of Jas Roux, which Le Fort (1973) considered to represent an important shear zone. It must, however, be stressed that the Jas Roux deposit is located over a deep-seated tectonic zone at the contact of the Ecrins anticline with the metamorphic series of the Sirac anticline.

Acknowledgements. The authors are indebted to Sir P. Skipwith, BRGM, for revising the English of this manuscript and for critical comments and to Prof. E. Marcoux, University of Orléans, for constructive review.

Submitted January 22, 2000

References

Bakken, B. M. – Einaudi, M. T. (1986): Spatial and temporal relations between wall rock alteration and gold mineralization, Main Pit, Carlin gold mine, Nevada, USA. – In: A. J. MacDonald ed.: Proceedings of Gold '86 symposium, Toronto, 1986, 388–403.

Balić-Žunić, T. – Šćavničar, T. S. – Engel, P. (1982): The crystal structure of rebulite $Tl_3Sb_5As_8S_{22}$. – Zeit. Krist., 160, 109–125.

Basu, K. – Bortnikov, N. S. – Mookherjee, A. – Mozgova, N. N. – Tsepin, A. I. – Vyal'sov, L. N. (1983): Rare minerals from Rajpura-Dariba, Rajasthan, India. IV: a new Pb-Ag-Tl-Sb sulfosalt, rayite. – N. Jhb. Mineral. Monatsh., (2), 296–304.

Berger, R. A. (1987): Crookesite and sabatierite in a new light - a crystallographer's comment. – Zeit. Krist., 181, 241–249.

Bracci, G. – Dalena, D. – Orlandi, P. – Duchi, G. – Vezzalini, G. (1980): Guettardite from Tuscany, Italy: a second occurrence. – Can. Mineral., 18, 13–15.

Brown, K. L. (1986): Gold deposition from geothermal discharges in New Zealand. – Econ. Geol., 81, 979–983.

Browne, P. R. L. (1969): Sulfide mineralization in a Broadlands geothermal drill hole, Taupo volcanic zone, New Zealand. – Econ. Geol., 64, 156–159.

Browne, P. R. L. (1971): Mineralisation in the Broadlands geothermal field, Taupo volcanic zone, New-Zealand. – Soc. Mining Geol. Japan, spec. issue 2, 64–75.

Browne, P. R. L. – Ellis, A. J. (1970): The Ohaki-Broadlands hydrothermal area, New-Zealand: mineralogy and related geochemistry. – Amer. J. Sci., 269, 97–131.

Browne, P. R. L. – Lovering, J. F. (1973): Composition of sphalerites from the Broadlands geothermal field and their significance to sphalerite geothermometry and geobarometry. – Econ. Geol., 68, 381–387.

Browne, P. R. L. – Lloyd, E. F. (1987): Water dominated geothermal systems and associated mineralization. In: Active volcanoes and geothermal systems, Taupo volcanic zone. – New Zealand Geological Survey record, 22, 85–152.

Burri, G. – Graeser, F. – Marumo, F. – Nowacki, W. (1965): Imhofit, ein neues Thallium-Arsensulfosalz aus dem Lengenbach (Binnatal, Kanton Wallis). – Chimia, 19, 499–500.

Caye, R. – Picot, P. – Pierrot, R. – Permingeat, F. (1967): Nouvelles données sur la vrbaïte, sa teneur en mercure. – Bull. Soc. fr. Minéral. Cristallogr., 90, 185–191.

Craig, J. R. – Chang, L. L. – Lees, W. R. (1973): Investigations in the Pb-Sb-S system. – Can. Mineral., 12, 199–206.

Cvetković, L. – Boronikhin, V. A. – Pavićević, M. K. – Krajnović, D. – Gržetić, I. – Libowitzky, E. – Giester, G. – Tillmans, E. (1995): Jankovicite, $Tl_5Sb_9(As,Sb)_4S_{22}$, a new Tl-sulfosalt from Allchar, Macedonia. – Mineral. Petrol., 53, 125–131.

Dickson, F. W. – Radtke, A. S. (1978): Weissbergite, $TlSbS_2$, a new mineral from the Carlin gold deposit, Nevada. – Amer. Mineral., 63, 720–724.

Dickson, F. W. – Radtke, A. S. – Peterson, J. A. (1979): Ellisite, Tl_3AsS_3, a new mineral from the Carlin gold deposit, Nevada, and associated sulfide and sulfosalt minerals. – Amer. Mineral., 64, 701–707.

Divjaković, V. – Nowacki, W. (1976): Die Kristallstruktur von Imhofit, $Tl_{5.6}As_{15}S_{25.3}$. – Zeit. Krist., 144, 323–333.

Edenharter, A. – Peters, T. (1979): Hydrothermalsynthese von Tl-haltigen Sulfosalzen. – Zeit. Krist., 150, 169–180.

Engel, P. (1980): Die Kristallstruktur von synthetischem Parapierrotit, $TlSb_5S_8$. – Zeit. Krist. 151, 203–216.

Engel, P. – Nowacki, W. – Balić-Žunić, T. – Šćavničar, S. (1982): The crystal structure of simonite $TlHgAs_3S_6$. – Zeit. Krist., 161, 159–166.

Engel, P. – Gostojić, M. – Nowacki, W. (1983): The crystal structure of pierrotite, $Tl_2(As,Sb)_{10}S_{16}$. – Zeit. Krist. 165, 209–215.

Eslinger, E. V. – Savin, S. M. (1973): Mineralogy and oxygen isotope geochemistry of the hydrothermally altered rocks of the Ohaki-Broadlands, New-Zealand geothermal area. – Amer. J. Sci., 273, 240–267.

Ewers, G. R. – Keays, R. R. (1977): Volatile and precious metal zoning in the Broadlands geothermal field, New Zealand. – Econ. Geol., 72, 1337–1354.

Garvin, P. L. (1973): Phase relations in the Pb-Sb-S system. – N. Jb. Miner. Abh. 118, 235–267.

Gatellier, J. P. – Marcoux, E. – Moëlo, Y. (1990): Nouvelle découverte de criddléite dans le district aurifère de Viges, Massif Central, Creuse, France. – Canad. Mineral., 28, 739–744.

Graeser, S. (1965): Die Mineralfundstellen in Dolomit des Binnatales. – Schweiz. Min. Petr. Mitt., 45, 597–795.

Graeser, S. (1988) Three new mineral species from the Binntal. – Uni Nova, 49: 17–19 (in German).

Gruzdev, V. S. – Chernitsova, N. M. – Shumakova, N. G. (1972): Aktashite, $Cu_6Hg_3As_5S_{12}$, new data. – Dokl. Akad. Nauk SSSR, 206, 694–697 (in Russian).

Guillemin, C. – Johan, Z. – Laforêt, C. – Picot, P. (1970): La pierrotite, $Tl_2(Sb,As)_{10}S_{17}$, une nouvelle espèce minérale. – Bull. Soc. fr. Min. Crist. 93, 66–71.

Harris, D. C. (1986): Mineralogy and geochemistry of the main Hemlo gold deposit, Hemlo, Ontario, Canada. – In: A. J. MacDonald ed., Proceedings of Gold '86 symposium, Toronto, 1986, 297–310.

Harris, D. C. – Roberts, A. C. – Laflamme, J. H. G. – Stanley, C. J. (1988): Criddleite, $TlAg_2Au_3Sb_{10}S_{10}$, a new gold-bearing mineral from Hemlo, Ontario, Canada. – Min. Mag., 52, 691–697.

Harris, D. C. – Roberts, A. C. (1989): Vaughanite, $TlHgSb_4S_7$, a new mineral from Hemlo, Ontario, Canada. – Min. Mag., 53, 79–83.

Ivanov, T. (1965): Zonal distribution of elements and minerals in the deposit Allchar. – In: Symposium Problems of postmagmatic ore deposition, Prague 1965, 2, 186–191.

Jambor, J. L. (1967): New lead sulfantimonides from Madoc, Ontario, Part 2 - mineral descriptions. – Canad. Mineral. 9, 191–213.

Jambor, J. L. – Plant, A. G. (1975): The composition of the lead sulphantimonide, robinsonite. – Can. Mineral. 13, 415–417.

Johan, Z. (1987): La crookesite, $TlCu_7Se_4$: nouvelles données et isotypie avec $NH_4Cu_7S_4$. – C. R. Acad. Sci. Paris, 304, 1121–1124.

Johan, Z. – Kvaček, M. (1971): La bukovite, $Cu_{3+x}Tl_2FeSe_{4-x}$, une nouvelle espèce minérale. – Bull. Soc. fr. Minéral. Cristallogr., 94, 529–533.

Johan, Z. – Pierrot, R. (1971): Smithite de Jas Roux. – Bull. Soc. fr. Min. Crist., 94, 565–569.

Johan, Z. – Pierrot, R. – Schubnel, H. J. – Permingeat, F. (1970): La picotpaulite, $TlFe_2S_3$, une nouvelle espèce minérale. – Bull. Soc. fr. Minéral. Cristallogr., 93, 545–549.

Johan, Z. – Mantienne, J. – Picot, P. (1974): La routhiérite, $TlHgAsS_3$ et la laffittite, $AgHgAsS_3$, deux nouvelles espèces minérales. – Bull. Soc. fr. Min. Crist., 97, 48–53.

Johan, Z. – Picot, P. – Hak, J. – Kvaček, M. (1975): La parapierrotire, un nouveau minéral thallifère d'Allchar (Yougoslavie). – Tschermaks Min. Petr. Mitt., 22, 200–210.

Johan, Z. – Kvaček, M. – Picot, P. (1978): La sabatierite, un nouveau séléniure de cuivre et de thallium. – Bull. Minéral., 101, 557–560.

Johan, Z. – Mantienne, P. – Picot, P. (1981): La chabournéite, un nouveau minéral thallifère. – Bull. Minéral., 104, 10–15.

Kaplunnik, L. N. – Pobedimskaya, E. A. – Belov, N. V. (1980): Crystal structure of aktashite ($Cu_6Hg_3As_4S_{12}$). – Dokl. Akad. Nauk SSSR, 251, 96–98 (in Russian).

Karup-Møller, S. (1978): Primary and secondary ore minerals associated with cuprostibite. – Bull. Grønlands Geol. Undersøgelse, 126, 23–45.

Kato, A. – Sakurai, K. I. – Ohsumi, K. (1970): An introduction to Japanese minerals. – Geol. Survey Japan, 1970, 92–93.

Kovalenker, V. A. – Laputina, I. P. – Evstigneeva, T. L. – Izoitko, V. M. (1976): Thalcusite, $Cu_{3-x}Tl_2Fe_{1+x}S_4$, a new thallium sulfide from copper-nickel ores of the Talnakh deposits. – Zap. Vses. Mineral. Obsch., 105, 202–206 (in Russian).

Kovalenker, V. A. – Laputina, I. P. – Semenov, Y. E. – Evstigneeva, T. L. (1978): Potassium-bearing thalcusite from the Ilímaussaq pluton and new data on chalcothallite. – Dokl. Akad Nauk SSSR, 239, 1203–1206 (in Russian).

Krupp, R. E. – Seward, T. M. (1987): The Rotokawa geothermal system, New Zealand: an active epithermal gold-depositing environment. – Econ. Geol., 82, 1109–1129.

Laurent, Y. – Picot, P. – Pierrot, R. – Ivanov, T. (1969): La raguinite, $TlFeS_2$, une nouvelle espèce minérale et le problème de l'allcharite. – Bull. Soc. fr. Minéral. Cristallogr., 92, 38–48.

Le Fort, P. (1973): Géologie du Haut Dauphiné cristallin (Alpes françaises). –Sciences de la Terre, mém. 25, 373 pp.

Le Fort, P. – Pecher, A. (1971): Présentation d'un schéma structural du Haut Dauphiné cristallin. – C. R. Acad. Sci. Paris, 273, 3–5.

Mantienne, J. (1974): La minéralisation thallifére de Jas Roux (Hautes-Alpes). – Unpubl. Thesis, Univ. Paris VI, 153 pp.

Marumo, F. – Burri, G. (1965): Nowackiite, a new copper-zinc arsenosulfosalt from Lengenbach (Binnatal, Kanton Wallis). – Chimia, 19, 500–501.

Mozgova, N. N. – Bortnikov, N. S. – Borodaev, Y. S. – Tzepine, A. I. (1982): Sur la non-stoechiométrie des sulfosels antimonieux arséniques de plomb. – Bull. Minéral., 105, 3–10.

Nagl, A. (1979): The crystal structure of a thallium sulfosalt, $Tl_8Pb_4Sb_{21}As_{19}S_{68}$. – Zeit. Krist., 150, 85–106.

Nakai, I. – Appelman, D. E. (1983): Laffittite, $AgHgAsS_3$; crystal structure and second occurrence from the Getchell mine, Nevada. – Amer. Mineral., 68, 235–244.

Nowacki, W. (1982): Isotypic state of aktashite ($Cu_6Hg_3As_4S_{12}$) and nowackiite ($Cu_6Zn_3As_4S_{12}$). – Kristallografiya, 27, 49–50 (in Russian).

Nowacki, W. – Bahezre, C. (1963): Die Bestimmung der chemischen Zusammensetzung einiger Sulfosalze aus dem Lengenbach (Binnatal, Kt. Wallis) mit Hilfe der elektronischen Mikrosonde. – Schweiz. Min. Petr. Mitt., 43, 407–411.

Nuffield, E. W. (1945): Studies on mineral sulfo-salts: X - andorite, ramdohrite and fizelyite. – Trans. Roy. Soc. Canada, ser. III, 39, 41–49.

Ohmasa, M. – Nowacki, W. (1971): The crystal structure of vrbaite, $Hg_3Tl_4As_8Sb_2S_{20}$. – Zeit. Krist., 134, 360–380.

Pašava, J. – Pertlik, F. – Stumpfl, E. F. – Zemann, J. (1989): Bernardite, a new thallium arsenic sulfosalt from Allchar, Macedonia, with a determination of the crystal structure. – Min. Mag., 53, 531–538.

Picot, P. – Johan, Z. (1983): Atlas of ore minerals. – BRGM-Elsevier ed., 458 pp.

Pierrot, R. – Picot, P. – Poulain, P. A. (1972): Inventaire minéralogique de la France, 05-Hautes-Alpes. – BRGM ed., 184 pp.

Radtke, A. S. – Dickson, F. W. (1975): Carlinite, Tl_2S, a new mineral from Nevada. – Amer. Mineral., 60, 559–565.

Radtke, A. S. – Dickson, F. W. – Slack, J. F. – Brown, K. L. (1977): Christite, a new thallium mineral from the Carlin deposit, Nevada. – Amer. Mineral., 62, 421–425.

Rudashevskii, N. S. – Karpenov, A. M. – Shipova, G. S. – Shishkin, N. N. – Ryabkin, V. A. (1979): Thalfenisite, the thallium analog of djerfisherite. – Zap. Vses. Min. Obsch., 108, 696–701 (in Russian).

Scott, J. D. – Nowacki, W. (1975): New data on wakabayashilite. – Can. Mineral., 13, 418–419.

Seeliger, E. (1954): Ein neues Vorkommen von Hutchinsonit in Wiesloch in Baden. – N. Jb. Min. Abh., 86, 163–178.

Semenov, E. I. – Sørensen, H. – Bezsmertnaya, M. S. – Novorossova, L. E. (1967): Chalcothallite, a new sulphide of copper and thallium from the Ilímaussaq alkaline intrusion, South Greenland. – Medd. Grønland, 181, 13–25.

Seward, T. M. (1973): Thio-complexes of gold and the transport of gold in hydrothermal ore solutions. – Geoch. Cosmoch. Acta, 37, 379–399.

Seward, T. M. – Kerrick, D. M. (1996): Hydrothermal CO_2 emission from the Taupo volcanic zone, New Zealand. – Earth and Planet. Sci. Lett., 139, 105–113.

Shannon, R. D. – Prewitt, C. T. (1970): Revised values of effective ion radii. – Acta Cryst., B 26, 1046–1048.

Simmons, S. F. – Browne, P. R. L. (1997): Saline fluid inclusions in sphalerite from the Broadlands-Ohaaki geothermal system: a coincidental trapping of fluids being boiled toward dryness. – Econ. Geol., 92, 485–489.

Skinner, B. J. – White, D. E. – Rose, H. J. – Mays, R. (1967): Sulfides associated with the Salton Sea geothermal brine. – Econ. Geol., 62, 316 –330.

Smith, G. F. – Prior, G. T. (1907): Red silver minerals from the Binnenthal, Switzerland. – Min. Mag., 14, 293 pp.

Solly, R. H. (1905): Some new minerals from the Binnenthal, Switzerland. – Min. Mag., 14, 74 pp.

Spiridonov, E. P. – Krapiva, L. Y. – Gapeev, A. K. – Stepanov, V. I. – Prushinskaya, E. Y. – Volgin, V. Y. (1981): Gruzdevite, $Cu_6Hg_3Sb_4S_{12}$, a new mineral from the Chauval antimony-mercury deposit, Central Asia. – Doklady Akad. Nauk SSSR, 261, 971–976 (in Russian).

Takéuchi, Y. – Ohmasa, M. – Nowacki, W. (1968): The crystal structure of wallisite, $PbTlCuAs_2S_5$, the Cu analogue of hatchite, $PbTlAgAs_2S_5$. – Zeit. Krist., 127, 349–365.

Vatin-Perignon, N. – Juteau, T. – Le Fort, P. (1973): Les filons du massif du Pelvoux. – Géol. alpine, 48, 207–227.

Vernet, J. (1965): La zone "Pelvoux-Argentera". – Bull. Serv. Carte géol. de la France, 60, N° 275, 294 pp.

Walia, D. S. – Chang, L. L. Y. (1973): Investigations in the systems PbS-Sb_2S_3-As_2S_3 and PbS-Bi_2S_3-As_2S_3. – Can. Mineral., 12, 113–119.

Weissberg, B. G. (1969): Gold silver ore-grade precipitates from New-Zealand thermal waters. – Econ. Geol., 64, 95–108.

White, D. E. (1965): Metal contents of some geothermal fluids. – In: Symposium Problems of postmagmatic ore deposition, Prague, 1965, 2, 432–443.

White, D. E. (1967): Mercury and base-metal deposits with associated thermal and mineral waters. – In: Geochemistry of Hydrothermal Ore Deposits, H. L. Barnes ed., 1st Ed., New York, 575–631.

White, D. E. (1968): Environments of generation of some base metal ore deposits. – Econ. Geol., 63, 301–335.

Wilson, J. R. – Robinson, P. D. – Wilson, P. N. – Stanger, L. W. – Salmon, G. L. (1991): Gillulyite, $Tl_2(As,Sb)_8S_{13}$, a new thallium arsenic sulfosalt from the Mercur gold deposit, Utah. – Amer. Mineral., 76, 653–656.

Wilson, J. R. – Gupta, S. P. K. – Robinson, P. D. – Criddle, A. J. (1993): Fengite, Tl_3AsS_4, a new thallium arsenic sulfosalt from the Mercur Au deposit, Utah, and revised optical data for gillulyite. – Amer. Mineral., 78, 1096–1103.

Thaliem bohaté zrudnění v Jas Roux, Hautem-Alpes, Francie: komplexní rudotvorný systém vázaný na sedimenty

Thaliem bohaté zrudnění vázané na sedimentární horniny v Jas Roux (Hautes-Alpes), Francie, které jsou tektonickými zbytky triasového pokryvu hercynských metamorfních sérií, vykazuje paragenetickou podobnost s geotermálními systémy existujícími v současné době na Novém Zélandě a v USA: (i) intenzivní silifikace okolních hornin a přítomnost aduláru, albitu, barytu a fluoritu; (ii) zvýšený obsah Li v silicifikovaných partiích; (iii) postupné obohacení rudotvorného systému těkavými prvky – Sb → Tl → Hg → As. Výskyt zrudnění je vázán na hlubokou tektonickou zónu tvořící kontakt mezi antiklinoriem Siracu a antiklinoriem des Ecrins, v jejíž blízkosti jsou v triasových sedimentech popsány basické vulkanity doprovázené tufy, jakož i rhyolitické výlevy. Je velice pravděpodobné, že mineralizace je vázána na jeden z těchto vulkanických projevů. Zrudnění je charakterizováno čtyřmi vývojovými stádii: (i) pyrit (0,07 % Tl) a sfalerit obsahující 0,7 % Fe, 0.8 % Cd, 0.1 % Tl; (ii) sulfosole Pb a Ag (twinnit, fáze $Pb_9Ag(As,Sb)_{13}S_{29}$, zinckenit, andorit) a antimonit; (iii) thaliové sulfosole (chabeourneit, pierrotit) a wakabazashilit; (iv) sulfosole bohaté na Ag, Hg, Tl a Cu (smithit, laffittit, routhierit, aktashit), realgar a následující neidentifikovatelné fáze: $Tl(As,Sb)_{10}S_{16}$, $Tl(Sb,As)_7S_{11}$ a Ag_2SbAsS_4. Jde nepochybně o jednu z geneticky nejzajímavějších thaliových mineralizací známých v současné době.